

The intrinsic shape of bulges

J. Méndez-Abreu^{1,2}, E. Simonneau³, J. A. L. Aguerri^{1,2}, E. M. Corsini⁴

¹*Instituto Astrofísico de Canarias, E-38200 La Laguna, Spain*

²*Departamento de Astrofísica, Universidad La Laguna, E-38205 La Laguna, Spain*

³*Institut d'Astrophysique de Paris, C.N.R.S.-U.P.M.C., F-75014 Paris, France*

⁴*Dipartimento di Astronomia, Università di Padova, I-35122 Padova, Italy*

(Received December , 2010)

The J -band structural parameters of a magnitude-limited sample of 148 unbarred S0–Sb galaxies were derived using the GASP2D algorithm and then analyzed to derive the intrinsic shape of their bulges. We developed a new method to derive the intrinsic shape of bulges based only on photometric data and on the geometrical relationships between the apparent and intrinsic shapes of bulges and disks. The method is conceived as completely independent of the studied class of objects, and it can be applied whenever a triaxial ellipsoid embedded in (or embedding) an axisymmetric component is considered. We found that the intrinsic shape is well constrained for a subsample of 115 bulges with favorable viewing angles. A large fraction of them is characterized by an elliptical section ($B/A < 0.9$). This fraction is 33%, 55%, and 43% if using their maximum, mean, or median equatorial ellipticity, respectively. Most of them are flattened along their polar axis ($C < (A+B)/2$). The distribution of triaxiality is strongly bimodal. This bimodality is driven by bulges with Sérsic index $n > 2$, or equivalently, by the bulges of galaxies with a bulge-to-total ratio $B/T > 0.3$. Bulges with $n \leq 2$ and with $B/T \leq 0.3$ follow a similar distribution, which is different from that of bulges with $n > 2$ and with $B/T > 0.3$. In particular, bulges with $n \leq 2$ and with $B/T \leq 0.3$ show a larger fraction of oblate axisymmetric (or nearly axisymmetric) bulges, a smaller fraction of triaxial bulges, and fewer prolate axisymmetric (or nearly axisymmetric) bulges with respect to bulges with $n > 2$ and with $B/T > 0.3$, respectively. According to predictions of the numerical simulations of bulge formation, bulges with $n \leq 2$, which show a high fraction of oblate axisymmetric (or nearly axisymmetric) shapes and have $B/T \leq 0.3$, could be the result of dissipational minor mergers. Both major dissipational and dissipationless mergers seem to be required to explain the variety of shapes found for bulges with $n > 2$ and $B/T > 0.3$.

KEY WORDS galaxies: bulges – galaxies: photometry – galaxies: statistics – galaxies: structure

1 Introduction

The intrinsic shapes of elliptical galaxies and disks have been extensively studied in the literature. However, bulges appear to be less studied, even if they account for about 25% of the stellar mass of the local universe [1].

The study of the intrinsic shape of bulges presents similarities, advantages, and drawbacks with respect to that of elliptical galaxies. For bulges, the problem is complicated by the presence of other luminous components and requires the accurate isolation of their light distribution. On the other hand, the presence of the galactic disk allows for the accurate constraining of the inclination of the bulge under the assumption that the two components share the same polar axis.

Although the kinematical properties of many bulges are well described by dynamical models of oblate ellipsoids which are flattened by rotation with little or no

anisotropy [2, 3, 4], the twisting of the bulge isophotes [5] and the misalignment between the major axes of the bulge and disk [6, 7] observed in several galaxies are not possible if the bulge and disk are both axisymmetric. These features were interpreted as the signature of bulge triaxiality. This idea is also supported by the presence of non-circular gas motions [8, 9, 10] and a velocity gradient along the galaxy minor axis [11, 12, 13]. Perfect axisymmetry is also ruled out when the intrinsic shape of bulges is determined by statistical analyses based on their observed ellipticities. Bertola et al. [6] measured the bulge ellipticity and the misalignment between the major axes of the bulge and disk in 32 S0–Sb galaxies. They found that these bulges are triaxial with mean axial ratios $\langle B/A \rangle = 0.86$ and $\langle C/A \rangle = 0.65$. In contrast, measurements of $\langle B/A \rangle = 0.79$ for the bulges of 35 early-type disk galaxies and $\langle B/A \rangle = 0.71$ for the bulges of 35 late-type spirals were found by Fathi & Peletier [14]. None of the 21 disk galaxies with morphological types between S0 and Sab studied by Noordermeer & van der Hulst [15] harbors a truly spherical bulge. They obtain a mean flattening $\langle C/A \rangle = 0.55$. Mosenkov et al. [16] obtained a median value of the flattening $\langle C/A \rangle = 0.63$ for a sample of both early and late-type edge-on galaxies in the near infrared.

In Méndez-Abreu et al. [7](Paper I) we measured the structural parameters of a sample of 148 unbarred early-to-intermediate spiral galaxies using the GASP2D algorithm to analyze their near-infrared surface-brightness distribution. The probability distribution function (PDF) of the bulge equatorial ellipticity was derived from the distributions of observed ellipticities of bulges and misalignments between bulges and disks. We proved that about 80% of the sample bulges are not oblate but triaxial ellipsoids with a mean axial ratio $\langle B/A \rangle = 0.85$.

In this work, (see Méndez-Abreu et al. [17] for details) we introduce a new method to derive the intrinsic shape of bulges under the assumption of triaxiality. This statistical analysis is based upon the analytical relations between the observed and intrinsic shapes of bulges and their surrounding disks and it is applied to the galaxy sample described in Paper I. The method make use only of photometric data and have been conceived to be completely independent of the studied class of objects, and it can be applied whenever triaxial ellipsoids embedded in (or embedding) an axisymmetric component are considered.

2 Basic geometrical considerations

We assume that the bulge is a triaxial ellipsoid and the disk is circular and lies in the equatorial plane of the bulge. Bulge and disk share the same center and polar axis. Therefore, the inclination of the polar axis (i.e., the galaxy inclination) and the position angle of the line of nodes (i.e., the position angle of the galaxy major axis) are directly derived from the observed ellipticity and orientation of the disk, respectively.

Let (x, y, z) be the Cartesian coordinates with the origin in the galaxy center, the x -axis and y -axis corresponding to the principal equatorial axes of the bulge, and the z -axis corresponding to the polar axis of the bulge and disk. If A , B , and

C are the lengths of the ellipsoid semi-axes (without considering $A \geq B \geq C$), the equation of the bulge in its own reference system is given by

$$\frac{x^2}{A^2} + \frac{y^2}{B^2} + \frac{z^2}{C^2} = 1. \quad (1)$$

Let (x', y', z') be now the Cartesian coordinates of the observer system. It has its origin in the galaxy center, the polar z' -axis along the line of sight (LOS) and pointing toward the galaxy. The plane of the sky lies on the (x', y') plane. The projection of the disk onto the sky plane is an ellipse whose major axis is the line of nodes (LON), i.e., the intersection between the galactic and sky planes. The angle θ between the z -axis and z' -axis corresponds to the inclination of the galaxy and therefore of the bulge ellipsoid; it can be derived as $\theta = \arccos(d/c)$ from the length c and d of the two semi-axes of the projected ellipse of the disk. We defined ϕ ($0 \leq \phi \leq \pi/2$) as the angle between the x -axis and the LON on the equatorial plane of the bulge (x, y) . Finally, we also defined ψ ($0 \leq \psi \leq \pi/2$) as the angle between the x' -axis and the LON on the sky plane (x', y') . The three angles θ , ϕ , and ψ are the usual Euler angles and relate the reference system (x, y, z) of the ellipsoid with that (x', y', z') of the observer by means of three rotations (Fig. 1). Indeed, because of the location of the LON is known, we can choose the x' -axis along it, and consequently it holds that $\psi = 0$. Now, if we identify the latter with the ellipse projected by the observed ellipsoidal bulge, we can determine the position of its axes of symmetry x_e and y_e and the lengths a and b of the corresponding semi-axes. The x_e -axis forms an angle δ with the LON corresponding to the x' -axis of the sky plane. We always choose $0 \leq \delta \leq \pi/2$ such that a can be either the major or the minor semi-axis. Later we will explain that this riddle is solved because the two possibilities coincide, and one is the mirror image of the other.

Following [18], we are able to express the length of the bulge semi-axes (A , B , and C) as a function of the length of the semi-axes of the projected ellipse (a , b) and the twist angle (δ).

$$A^2 = K^2 \left(1 + \frac{e \sin 2\delta \tan \phi}{1 + e \cos 2\delta \cos \theta} \right), \quad (2)$$

$$B^2 = K^2 \left(1 - \frac{e \sin 2\delta \cot \phi}{1 + e \cos 2\delta \cos \theta} \right), \quad (3)$$

$$C^2 = K^2 \left(1 - \frac{2e \cos 2\delta}{\sin^2 \theta (1 + e \cos 2\delta)} + \frac{2e \cos \theta \sin 2\delta}{\sin^2 \theta (1 + e \cos 2\delta)} \cot^2 \phi \right). \quad (4)$$

where $K^2 = \frac{a^2 + b^2}{2} [1 + e \cos 2\delta]$, and $e = \frac{a^2 - b^2}{a^2 + b^2}$. The values of a , b , δ , and θ can be directly obtained from observations. Unfortunately, the relation between the intrinsic and projected variables also depends on the spatial position of the bulge (i.e., on the ϕ angle), which is actually the unique unknown of our problem. Indeed, this will constitute the basis of our statistical analysis.

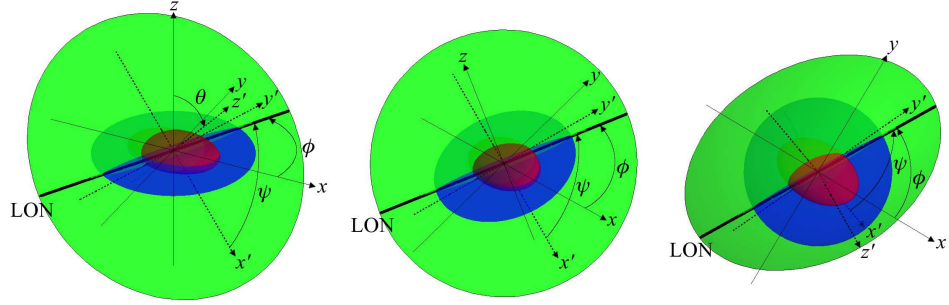


Figure 1: Schematic three-dimensional view of the ellipsoid geometry. The bulge ellipsoid, the disk plane, and the sky plane are shown in red, blue, and green, respectively. The reference systems of the ellipsoid and of the observer as well as the LON are plotted with thin solid lines, thin dashed lines, and a thick solid line, respectively. The bulge ellipsoid is shown as seen from an arbitrary viewing angle (left panel), along the LOS (central panel), and along the polar axis (right panel).

2.1 Characteristic angles

There are physical constraints which limit the possible values of ϕ , such as the positive length of the three semi-axes of the ellipsoid [18]. Therefore, we define some characteristic angles which constrain the range of ϕ . Two different possibilities must be taken into account for any value of the observed variables a , b , δ and θ .

The first case corresponds to $a > b$. It implies that $e > 0$ and $A > B$. For any value of ϕ , $A^2 > K^2$ and K^2 is always a positive value. On the other hand, B^2 and C^2 can be either positive or negative depending on the value of ϕ . This limits the range of the values of ϕ . B^2 is positive only for $\phi > \phi_B$. The angle ϕ_B is defined by $B^2 = 0$ in Eq. 3 as

$$\tan \phi_B = \frac{e \sin 2\delta}{\cos \theta (1 + e \cos 2\delta)}. \quad (5)$$

Likewise, C^2 is positive only for values of $\phi < \phi_C$. The angle ϕ_C is defined by $C^2 = 0$ in Eq. 4 as

$$\tan 2\phi_C = \frac{2e \sin 2\delta \cos \theta}{e \cos 2\delta (1 + \cos^2 \theta) - \sin^2 \theta}. \quad (6)$$

Thus, if $a > b$ then the values of ϕ can only be in the range $\phi_B \leq \phi \leq \phi_C$.

The second case corresponds to $a < b$. It implies that $e < 0$ and $A < B$. For any value of ϕ , $B^2 > K^2$ and K^2 is always a positive value. But, A^2 and C^2 can be either positive or negative depending on the value of ϕ . This limits the range of the values of ϕ . A^2 is positive only for $\phi < \phi_A$. The angle ϕ_A is defined by $A^2 = 0$ in Eq. 2 as

$$\tan \phi_A = -\frac{\cos \theta (1 + e \cos 2\delta)}{e \sin 2\delta}. \quad (7)$$

Likewise, C^2 is positive only for values of $\phi > \phi_C$. The angle ϕ_C is given in Eq. 6. Thus, if $a < b$, then the values ϕ can only be in the range $\phi_C \leq \phi \leq \phi_A$.

However, the problem is symmetric: the second case, when the first semi-axis of the observed ellipse corresponds to the minor axis (i.e., $a < b$), is the mirror situation of the first case, when the first measured semi-axis of the observed ellipse corresponds to the major axis (i.e., $a > b$). In the second case, if we assume the angle $\pi/2 - \delta$ to define the position of the major semi-axis a of the observed ellipse with respect to the LON in the sky plane, and $\pi/2 - \phi$ to define the position of the major semi-axis A of the equatorial ellipse of the bulge with respect to the LON in the bulge equatorial plane, then we can always consider $a > b$ and $A > B$. Therefore, $e \geq 0$ and $E \geq 0$ always. This means that we have the same mathematical description in both cases: the possible values of ϕ are $\phi_B \leq \phi \leq \phi_C$ with ϕ_B and ϕ_C defined by Eqs. 5 and 6, respectively. According to this definition oblate and prolate triaxial ellipsoids do not necessarily have an axisymmetric shape. A detailed description of all these cases will be given at the end of this section.

We define the quadratic mean radius of the equatorial ellipse of the bulge in order to extensively discuss all the different possibilities.

$$R^2 = \frac{A^2 + B^2}{2} = K^2 \tan \phi_B [\cot \phi_B - \cot 2\phi], \quad (8)$$

which depends only on the unknown position ϕ .

Since $A^2 > B^2$, $A^2 \geq R^2 \geq B^2$ but there is always a value ϕ_{RC} corresponding to the case $C^2 = R^2$

$$\tan 2\phi_{RC} = \tan 2\delta \frac{1 + \cos^2 \theta}{2 \cos \theta}. \quad (9)$$

The mean equatorial radius allows us to distinguish oblate ($C^2 < R^2$) and prolate ($C^2 > R^2$) triaxial ellipsoids. Unfortunately, the situation is more complicated due to the existence of other intermediate angles such as ϕ_{BC} which occurs when $B^2 = C^2$ and ϕ_{AC} which occurs when $A^2 = C^2$. In particular, there are four different possibilities for the intrinsic shape of the bulge ellipsoid. They are sketched in Fig. 2 and can be described as follows

- If $\phi_{AC} < \phi_{RC} < \phi_B$ the triaxial ellipsoid is always oblate (Fig. 2, left panel). It is either completely oblate (i.e., $A > B > C$) if $R > B > C$ ($\phi_{BC} < \phi < \phi_C$) or partially oblate if $R > C > B$ ($\phi_B < \phi < \phi_{BC}$).
- If $\phi_{AC} < \phi_B < \phi_{RC}$ the triaxial ellipsoid can be either oblate or prolate (Fig. 2, central panel). It is either completely oblate if $R > B > C$ ($\phi_{BC} < \phi < \phi_C$), or partially oblate if $R > C > B$ ($\phi_{RC} < \phi < \phi_{BC}$), or partially prolate if $C > R > B$ ($\phi_B < \phi < \phi_{RC}$).

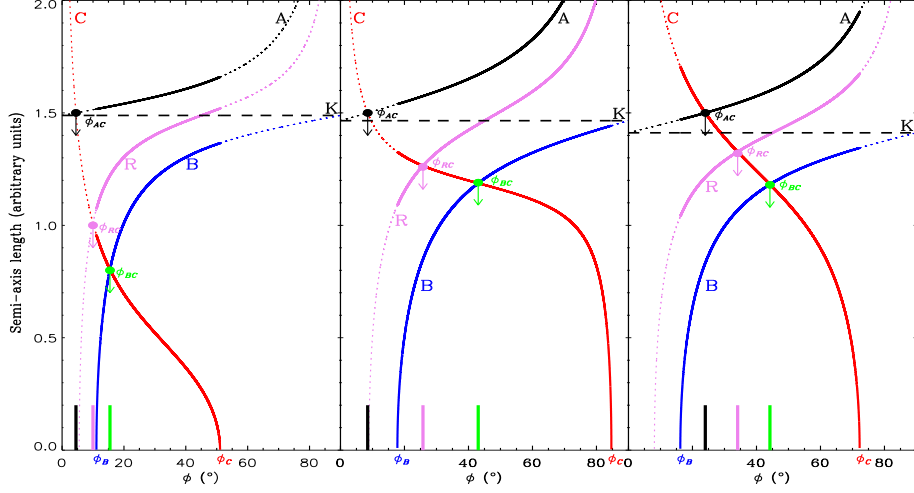


Figure 2: The lengths A , B , and C of the semi-axes of the bulge ellipsoid and its mean equatorial radius R as a function of the angle ϕ . The solid lines correspond to the ranges of physically possible values of A , B , C , and R , while the dotted lines show their overall trends within $0 \leq \phi \leq \pi/2$. A triaxial bulge with $\phi_{AC} < \phi_{RC} < \phi_B$, $\phi_{AC} < \phi_B < \phi_{RC}$, and $\phi_B < \phi_{AC} < \phi_{RC}$ is shown in the left, central, and right panel, respectively.

- If $\phi_B < \phi_{AC} < \phi_{RC}$ four different possibilities are allowed for the triaxial shape of the bulge ellipsoid (Fig. 2, right panel). It is either completely oblate if $R > B > C$ ($\phi_{BC} < \phi < \phi_C$), or partially oblate if $R > C > B$ ($\phi_{RC} < \phi < \phi_{BC}$), or partially prolate if $A > C > R$ ($\phi_{AC} < \phi < \phi_{BC}$), or completely prolate (i.e., $C > A > B$) if $C > A > R$ ($\phi_B < \phi < \phi_{AC}$).

3 Intrinsic shape of bulges

The strength of this new method is that now we are able to constraint the shape of bulges within well defined range of axis ratios, and, moreover, since the axis ratios are given by a probability distribution function, a complete 3D dimensional picture of their shape can be obtained. The equation linking the intrinsic ellipticity and flattening axis ratio is given by

$$\frac{2 \sin(2\phi_C) C^2}{F_\theta A^2} = \sin(2\phi_C - \phi_B) \sqrt{\left(1 - \frac{B^2}{A^2}\right)^2 - \sin^2 \phi_B \left(1 + \frac{B^2}{A^2}\right)^2} - \sin \phi_B \cos(2\phi_C - \phi_B) \left(1 + \frac{B^2}{A^2}\right)^2. \quad (10)$$

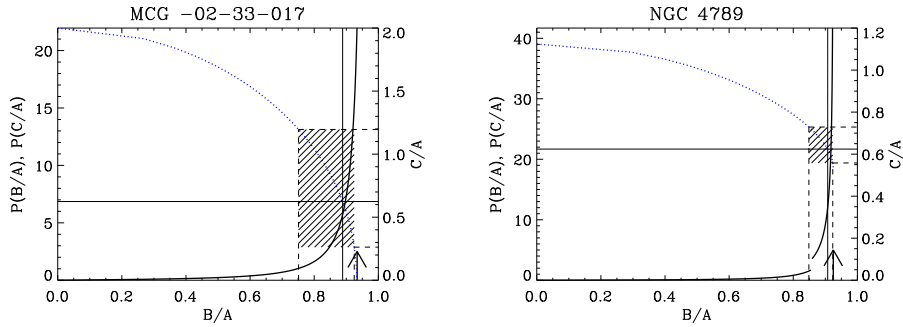


Figure 3: Relation between the axial ratios B/A and C/A for two sample bulges. MCG -02-33-017 (left panel) hosts a bulge with $\phi_M < \phi_C$ and NGC 4789 (right panel) hosts a bulge with $\phi_M > \phi_C$. The probability associated with each value of B/A and its corresponding value of C/A (thick solid line), the value of C/A as a function of B/A (dotted line), the maximum value of the equatorial ellipticity (arrow), the median values of B/A (vertical thin solid line) and C/A (horizontal thin solid line), and the confidence region which encloses all the possible values of B/A and C/A within a 67% probability (hatched area) are shown in both panels.

which constrain the intrinsic shape of an observed bulge with the help of the known characteristic angles ϕ_B and ϕ_C , which depend only on the measured values of a , b , δ , and θ .

Since B/A and C/A are both functions of the same variable ϕ , their probabilities are equivalent (i.e., for a given value of B/A with probability $P(B/A)$, the corresponding value of C/A obtained by Eq. 10 has a probability $P(C/A) = P(B/A)$). This allows us to obtain the range of possible values of B/A and C/A for an observed bulge and to constrain its most probable intrinsic shape. An example of the application of Eq. 10 to two bulges of our sample is shown in Fig. 3. The intrinsic shape of bulges for bulges with $\phi_C < \phi_M = \frac{\pi}{4} + \frac{\phi_B}{2}$ is less constrained, since the median values of B/A and C/A are less representative of their actual values. This is the case for the bulge of MCG -02-33-017 (Fig. 3, left panel). On the contrary, the intrinsic shape of bulges with $\phi_C > \phi_M$ is better constrained. This is the case for the bulge of NGC 4789 (Fig. 3, right panel).

3.1 Statistics of the intrinsic shape of bulges

We derived the triaxiality parameter, as defined by [19] $T = \frac{1 - \left(\frac{\hat{B}}{\hat{A}}\right)^2}{1 - \left(\frac{\hat{C}}{\hat{A}}\right)^2}$, for the 115 sample bulges with a well-constrained intrinsic shape (i.e., those with $\phi_C > \phi_M$). \hat{A} , \hat{B} , and \hat{C} are the lengths of the longest, intermediate, and shortest semi-axes of the triaxial ellipsoid, respectively (i.e., $\hat{A} \geq \hat{B} \geq \hat{C}$). This notation is different with respect to that we adopted in the previous sections. Now prolate bulges do either

lie on the disk plane (and are similar to bars) or do stick out from the disk (and are elongated perpendicularly to it). This change of notation is needed to compare our results with those available in literature.

The triaxiality parameter for bulges with $\phi_C > \phi_M$ is characterized by a bimodal distribution with a minimum at $T = 0.55$ and two maxima at $T = 0.05$ and $T = 0.85$, respectively. According to this distribution, $65\% \pm 4\%$ of the selected bulges are oblate triaxial (or axisymmetric) ellipsoids ($T < 0.55$) and the remaining $35\% \pm 4\%$ are prolate (or axisymmetric) triaxial ellipsoids ($T \geq 0.55$).

We investigated the cause of such a bimodality by separating the bulges according to their Sérsic index (n) and bulge-to-total luminosity ratio (B/T). Both quantities were derived for each sample bulge in Paper I. The bimodality is driven by bulges with Sérsic index $n > 2$, or alternatively, by bulges of galaxies with $B/T > 0.3$. We find that $66\% \pm 4\%$ of bulges with $n > 2$ have $T < 0.55$. Their number decreases as T increases from 0 to 0.55. The remaining bulges have $T > 0.55$ and their number increases as T ranges from 0.55 to 1. A similar distribution is observed for the bulges of galaxies with $B/T > 0.3$. $67\% \pm 4\%$ of them host a bulge with $T < 0.55$. Instead, the distribution of the triaxiality parameter of bulges of galaxies with $B/T \leq 0.3$ is almost constant with a peak at $T = 0.05$. This is true also for the bulges with $n \leq 2$, although to a lesser degree. The two subsamples of bulges with $n \leq 2$ and $n > 2$ are different, as confirmed by a Kolmogorov-Smirnov test (99% confidence level). In particular, the fraction of oblate axisymmetric (or nearly axisymmetric) bulges ($T < 0.1$) is remarkably higher for $n \leq 2$ ($27\% \pm 4\%$) than for $n > 2$ ($14\% \pm 3\%$). The fraction of triaxial bulges ($0.1 \leq T \leq 0.9$) is lower for $n \leq 2$ ($71\% \pm 5\%$) than for $n > 2$ ($76\% \pm 3\%$). The fraction of prolate axisymmetric (or nearly axisymmetric) bulges ($T > 0.9$) for $n \leq 2$ is $2\% \pm 2\%$, but $11\% \pm 3\%$ for $n > 2$. The two subsamples of bulges of galaxies with $B/T > 0.3$ and $B/T \leq 0.3$ are different too, as confirmed by a Kolmogorov-Smirnov test (99% confidence level). The distribution of bulges with $n \leq 2$ and bulges of galaxies with $B/T \leq 0.3$ appears to be the same at a high confidence level ($> 99\%$) as confirmed by a Kolmogorov-Smirnov test.

Bulges with $\phi_C > \phi_M$ can be divided into two classes: those with $n \leq 2$ (or $B/T \leq 0.3$) and those with $n > 2$ (or $B/T > 0.3$). About 70% of bulges with $n \leq 2$ are hosted by galaxies with $B/T \leq 0.3$. The same is true for bulges with $n > 2$ which are mostly hosted by galaxies with $B/T > 0.3$. This agrees with the correlation between n and B/T .

4 Conclusions

In this work, we have developed a new method to derive the intrinsic shape of bulges. It is based upon the geometrical relationships between the observed and intrinsic shapes of bulges and their surrounding disks. We assumed that bulges are triaxial ellipsoids with semi-axes of length A and B in the equatorial plane and C along the polar axis. The bulge shares the same center and polar axis of its disk, which is circular and lies on the equatorial plane of the bulge. The intrinsic shape of the bulge

is recovered from photometric data only. They include the lengths a and b of the two semi-major axes of the ellipse, corresponding to the two-dimensional projection of the bulge, the twist angle δ between the bulge major axis and the galaxy line of nodes, and the galaxy inclination θ . The method is completely independent of the studied class of objects, and it can be applied whenever a triaxial ellipsoid embedded in (or embedding) an axisymmetric component is considered.

We analyzed the magnitude-limited sample of 148 unbarred S0–Sb galaxies, for which we have derived (Paper I) their structural parameters by a detailed photometric decomposition of their near-infrared surface-brightness distribution.

We derived the triaxiality parameter, as defined by [19], for all of them. We found that it follows a bimodal distribution with a minimum at $T = 0.55$ and two maxima at $T = 0.05$ (corresponding to oblate axisymmetric or nearly axisymmetric ellipsoids) and $T = 0.85$ (strongly prolate triaxial ellipsoids), respectively. This bimodality is driven by bulges with Sérsic index $n > 2$ or alternatively by bulges of galaxies with a bulge-to-total ratio $B/T > 0.3$. Bulges with $n \leq 2$ and bulges of galaxies with $B/T \leq 0.3$ follow a similar distribution, which is different from that of bulges with $n > 2$ and bulges of galaxies with $B/T > 0.3$.

The different distribution of the intrinsic shapes of bulges according to their Sérsic index gives further support to the presence of two bulge populations with different structural properties: the classical bulges, which are characterized by $n > 2$ and are similar to low-luminosity elliptical galaxies, and pseudobulges, with $n \leq 2$ and characterized by disk-like properties. The correlation between the intrinsic shape of bulges with $n \leq 2$ and those in galaxies with $B/T \leq 0.3$ and between bulges with $n > 2$ and those in galaxies with $B/T > 0.3$ agrees with the correlation between the bulge Sérsic index and bulge-to-total ratio of the host galaxy, as recently found by [20] and [21].

The observed bimodal distribution of the triaxiality parameter can be compared to the properties predicted by numerical simulations. [22] studied the structure of spheroidal remnants formed from major dissipationless and dissipational mergers of disk galaxies. Dissipationless remnants are triaxial with a tendency to be more prolate, whereas dissipational remnants are triaxial and tend to be much closer to oblate. In addition, [23] used semi-empirical models to predict galaxy merger rates and contributions to bulge growth as functions of merger mass, redshift, and mass ratio. They found that high B/T systems tend to form in major mergers, whereas low B/T systems tend to form from minor mergers. In this framework, bulges with $n \leq 2$, which shows a high fraction of oblate axisymmetric (or nearly axisymmetric) shapes and have $B/T \leq 0.3$, could be the result of dissipational minor mergers. A more complex scenario including both major dissipational and dissipationless mergers is required to explain the variety of intrinsic shapes found for bulges with $n > 2$ and $B/T > 0.3$.

However, high-resolution numerical simulations in a cosmologically motivated framework that resolves the bulge structure are still lacking. The comparison of a larger sample of bulges with a measured intrinsic shape and covering the entire Hubble sequence with these numerical experiments is the next logical step in addressing the issue of bulge formation.

References

- [1] Driver, S. P., Allen, P. D., Liske, J., & Graham, A. W. 2007, *ApJL*, 657, L85
- [2] Davies, R. L. & Illingworth, G. 1983, *ApJ*, 266, 516
- [3] Corsini, E. M., Pizzella, A., Sarzi, M., et al. 1999, *A&A*, 342, 671
- [4] Pignatelli, E., Corsini, E. M., Vega Beltrán, J. C., et al. 2001, *MNRAS*, 323, 188
- [5] Zaritsky, D. & Lo, K. Y. 1986, *ApJ*, 303, 66
- [6] Bertola, F., Vietri, M., & Zeilinger, W. W. 1991, *ApJL*, 374, L13
- [7] Méndez-Abreu, J., Aguerri, J. A. L., Corsini, E. M., & Simonneau, E. 2008, *A&A*, 478, 353
- [8] Gerhard, O. E. & Vietri, M. 1986, *MNRAS*, 223, 377
- [9] Falcón-Barroso, J., Bacon, R., Bureau, M., et al. 2006, *MNRAS*, 369, 529
- [10] Pizzella, A., Corsini, E. M., Sarzi, M., et al. 2008, *MNRAS*, 387, 1099
- [11] Corsini, E. M., Pizzella, A., Coccato, L., & Bertola, F. 2003, *A&A*, 408, 873
- [12] Coccato, L., Corsini, E. M., Pizzella, A., et al. 2004, *A&A*, 416, 507
- [13] Coccato, L., Corsini, E. M., Pizzella, A., & Bertola, F. 2005, *A&A*, 440, 107
- [14] Fathi, K. & Peletier, R. F. 2003, *A&A*, 407, 61
- [15] Noordermeer, E. & van der Hulst, J. M. 2007, *MNRAS*, 376, 1480
- [16] Mosenkov, A. V., Sotnikova, N. Y., & Reshetnikov, V. P. 2010, *MNRAS*, 401, 559
- [17] Méndez-Abreu, J., Simonneau, E., Aguerri, J. A. L., & Corsini, E. M. 2010, *A&A*, 521, 71
- [18] Simonneau, E., Varela, A. M., & Munoz-Tunon, C. 1998, *Nuovo Cimento B Serie*, 113, 927
- [19] Franx, M., Illingworth, G., & de Zeeuw, T. 1991, *ApJ*, 383, 112
- [20] Drory, N. & Fisher, D. B. 2007, *ApJ*, 664, 640
- [21] Fisher, D. B. & Drory, N. 2008, *AJ*, 136, 773
- [22] Cox, T. J., Dutta, S. N., Di Matteo, T., et al. 2006, *ApJ*, 650, 791
- [23] Hopkins, P. F., Bundy, K., Croton, D., et al. 2010, *ApJ*, 715, 202